Journal of Magnetism and Magnetic Materials 381 (2015) 337–343

Contents lists available at ScienceDirect

Journal of Magnetism and Magnetic Materials

journal homepage: www.elsevier.com/locate/jmmm

Experimental determination of the critical Rayleigh number for thermomagnetic convection with focus on fluid composition

M. Heckert, L. Sprenger *, A. Lange, S. Odenbach

TU Dresden, Chair of Magnetofluiddynamics, Measuring and Automation Technology, 01062 Dresden, Germany

ARTICLE INFO

Article history:
Received 3 December 2014
Received in revised form
8 January 2015
Accepted 8 January 2015
Available online 12 January 2015

Keywords:
Thermomagnetic convection
Magnetic fluids
Magnetic Rayleigh number

ABSTRACT

Thermomagnetic convection has been investigated for two kerosene-based magnetic fluids (EMG 905 and NF4000C) with a focus on the determination of the critical Rayleigh numbers for the onset of convective instability in a fluid layer. A comparison with published data for the ester-based APG 513A-fluid and theoretical predictions yield similar critical magnetic Rayleigh numbers for the EMG and APG-fluids around $Ra_{m,c} \approx 2500$, which is near the expected value, but $Ra_{m,c} = 856$ for the NF-fluid. As the latter differs from the other two fluids mainly in the particle size distribution, it is assumed that the size of the particles has an important and yet uninvestigated impact on the convective behavior of magnetic fluids.

1. Introduction

Thermomagnetic convection is a transport phenomenon in magnetic fluids. Its driving force is a magnetization gradient in a layer of fluid imposed by a temperature gradient. The status of the stability of the fluid can, analogue to buoyancy-driven convection, be described by a magnetic Rayleigh-number

$$Ra_m = \frac{\mu_0 K^2 \Delta T^2 d^2}{\eta\kappa(1+\chi)}, \tag{1}$$

which was introduced by Finlayson [1]. Here μ_0 denotes the vacuum permeability, K the pyromagnetic coefficient, ΔT the temperature difference across the layer of fluid, d the thickness of the layer, η the dynamic viscosity of the fluid, κ its temperature diffusivity, and χ its susceptibility. Convection will set in if that number exceeds a critical value $Ra_{m,c}$. According to Finlayson [1], this value depends on χ and a magnetic factor $M_3 = (1 + M/H_i)/(1+\chi)$ which includes the magnetization M and the inner magnetic field H_i of the fluid. Values of $Ra_{m,c}$ for the region of interest of the fluids investigated in this work are printed Fig. 1.

The existence of pure thermomagnetic convection was experimentally proven by Odenbach [2] under microgravity conditions. However, under normal gravity conditions a vertical temperature gradient across a horizontal layer of fluid always results in buoyancy forces which can destabilize the fluid when heated from below and stabilize it when heated from above. According to Chandrasekhar [3], these forces can be characterized by the Rayleigh-number

$$Ra = \frac{\beta g \rho \Delta T d^3}{\eta\kappa}, \tag{2}$$

where β denotes the thermal expansion coefficient and ρ is the density of the fluid. In a fluid layer constrained between two rigid boundaries, pure thermal convection sets in if the Rayleigh-number exceeds $Ra_c = 1708$. To take both driving forces into account, Finlayson [1] assumed that convective instability in a layer of fluid sets in for

$$\frac{Ra}{Ra_c} + \frac{Ra_m}{Ra_{m,c}} \geq 1. \tag{3}$$

With Eqs. (1)–(3) it is possible to determine the critical temperature difference ΔT_c for the onset of convection as a function of the critical magnetic and thermal Rayleigh numbers as

$$\Delta T_c = -\frac{Ra_{m,c}}{Ra_c}\cdot A \pm \sqrt{\left(\frac{Ra_{m,c}}{Ra_c}\cdot A\right)^2 + Ra_{m,c}\cdot B}$$

$$\text{with:} \quad A = \frac{\beta\cdot g\cdot\rho\cdot d\cdot(1+\chi)}{2\cdot\mu_0\cdot K^2} \quad \text{and} \quad B = \frac{\kappa\cdot\nu\cdot(1+\chi)}{\mu_0\cdot d^2\cdot K^2}. \tag{4}$$

Experiments, where buoyancy and thermomagnetic forces are present, have been carried out for example by Schwab [4,5] and Engler [6–8], but nonetheless the critical magnetic Rayleigh number is still not well described and might be dependent on the fluid's composition.

Beside the theoretical investigations done by Finlayson [1],

* Corresponding author.
E-mail address: Lisa.Sprenger@tu-dresden.de (L. Sprenger).

http://dx.doi.org/10.1016/j.jmmm.2015.01.014
0304-8853/

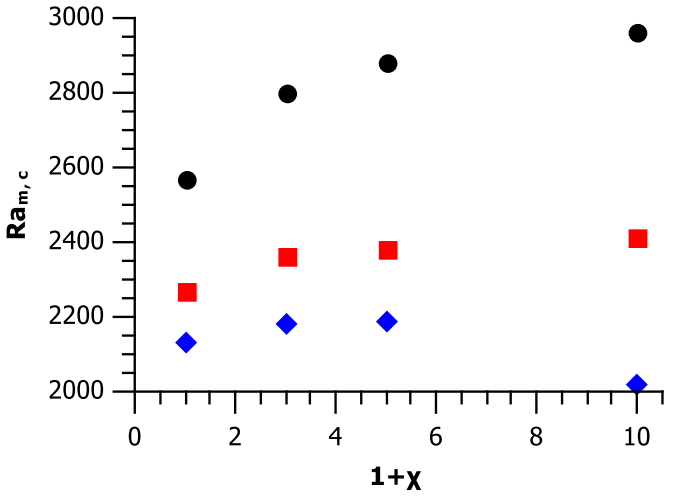

Fig. 1. $Ra_{m,c}$ as a function of $(1+\chi)$ for $M_3 = 1$ (•), $M_3 = 2$ (□) and $M_3 = 3$ (◇) from [1].

further theoretical studies have been carried out by Huke et al. [9] and Laroze et al. [10]. These works in contrast to Finlaysons work [1] do not concentrate on the onset of convection but focus on different pattern formations while convection is present. Further experimental investigations have been carried out by Berkovsky et al. [11]. These focus on convection in a vertical layer of fluid and can therefore not be compared concisely with the new investigations presented within this paper.

For these reasons a large series of convection experiments on magnetic fluids has been performed with the experimental setup built by Engler [6–8]. Namely the EMG 905-fluid and the NF4000C-fluid, both kerosene-based magnetite fluids manufactured by Ferrotec (Santa Clara, USA), are investigated at various magnetic field strengths and temperature differences.

2. Experimental setup

All experiments have been performed in a convection cell built by Engler, which is described in detail in [6,7] and sketched Fig. 2. On account of the opacity of magnetic fluids, the onset of convection is determined via the heat flux across the layer of fluid, which is expected to increase with the onset of convective motion in the fluid. The fluid is constrained in a horizontal cylindrical gap with a diameter of 88 mm and a height of 2–5.5 mm between two copper plates on each side. Two–three thermistors in each copper plate are used to measure the temperature difference over the fluid gap. A heat flux sensor is positioned inbetween the lower pair of copper plates.

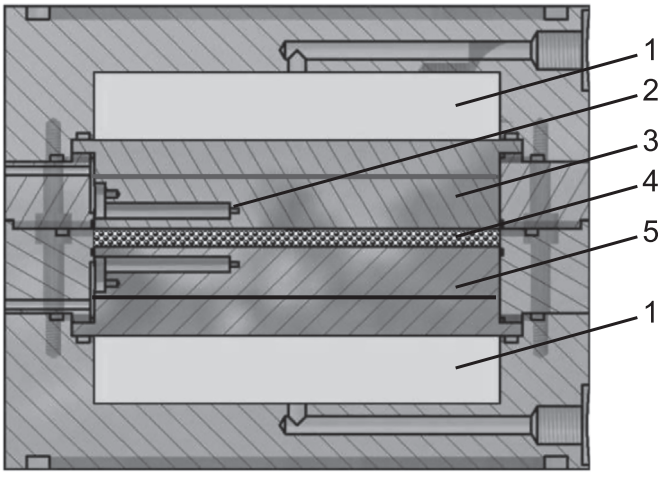

Fig. 2. Sketch of the fluid cell built by Engler [6,7]. (1) Water reservoir, (2) thermistor, (3) copper plates, (4) magnetic fluid, and (5) copper plates with heat flux sensor in between.

The temperature gradient is imposed by two water reservoirs flanking the outer copper plates. In a convection experiment both reservoirs are initially held at 313.15 K for about 3 h. Then one reservoir is cooled down and the other one is heated up, both in steps of 1 K if not otherwise stated in this paper. The temperature is kept constant for 32 min at each step prior to the data recording. The latter itself takes 3 min. The total of 36 steps leads to a maximum temperature difference of 70 K between the water reservoirs, which results in a maximum temperature difference of 30–40 K over the layer of fluid.

The magnetic field is applied perpendicular to the fluid layer by two pairs of Helmholtz-coils in a Fanselau configuration [12]. The larger coils are positioned concentric and equally distanced between the two smaller ones. The fluid layer's center point is placed on the center point of the group of the four coils.

A typical experimental output is shown Fig. 3, detected for the EMG 905-fluid with a layer thickness of 2 mm. The heat flux density shown there is a direct record of the heat flux sensor, scaled with the cross-sectional area of the layer. The heat flux values are corrected by subtracting the heat flux which arises from heat loss to the environment at the cell's outer wall between the heat flux sensor and the fluid layer. These values are obtained by detecting the heat flux while applying identical temperatures at the upper and lower layer's boundaries. For a temperature of about 280 K a loss of -0.5 W is determined, while for 350 K approximately 2 W can be detected.

The Nusselt number ($Nu = \alpha h/(\lambda)$) in Fig. 3 is calculated using the thermal conductivity λ of the fluid without magnetic field, the height of the fluid layer h, and $\alpha = \dot{q}/\Delta T$, with $\dot{q}$ being the heat flux density in W/m^2. Values for its calculation are shown in Section 3 (Fluid characterization). In both plots an abrupt change in slope of the signal is visible. This is assumed to stand for the onset of convection while leaving the conductive state of heat transfer. The critical temperature difference ΔT_c is defined as the intersection of linear fits of the heat flux density in the conductive and convective section, neglecting 3–4 data points inbetween, where transition takes place.

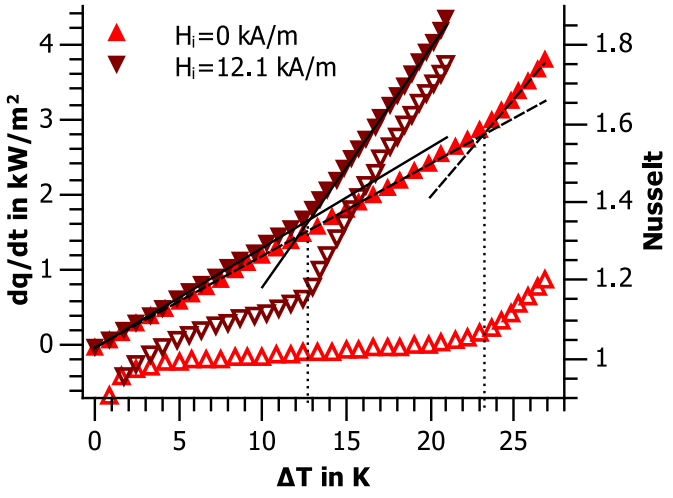

Fig. 3. Heat flux density $\dot{q}$ (filled symbols) and Nusselt number (open symbols) of EMG 905-fluid when heated from below with and without magnetic field H_i. Lines mark the linear fits of conductive and convective state leading to the critical temperature difference.

3. Fluid characterization

Two kerosene-based magnetic fluids manufactured by Ferrotec (Santa Clara, USA) have been investigated: EMG 905-fluid which was also used by Schwab [4] and NF4000C-fluid, a similar fluid with smaller particles. In order to calculate the limit of stability, a comprehensive characterization of these fluids is necessary. The results are shown Table 1 and in Figs. 4–7. As the results are later being compared with Engler [6–8], the parameters of the ester-based APG 513A-fluid (Ferrotec, Santa Clara, USA) investigated in that work are presented here as well.

A pyknometer (Brand, $V = 5.347\ \mathrm{m}^3$ at 293 K) was used for the determination of the fluids' densities ρ and thermal expansion coefficients β between 293 K and 333 K.

The heat capacity C_p was calculated using a mixing rule of the specific heat capacities of magnetite ($C_{p,Fe_3O_4} = 669\ \mathrm{J/kg\,K}$ at 313 K [13]) and kerosene ($C_{p,kerosene} = 2050\ \mathrm{J/kg\,K}$ at 314 K [14]): $C_p = \omega_{Fe_3O_4} \cdot C_{p,Fe_3O_4} + \omega_{kerosene} \cdot C_{p,kerosene}$, where ω denotes the mass percentage of magnetite or kerosene. Its validity for similar magnetic fluids was proven by Higano et al. [15]. Here it is assumed that the fluid only consists of magnetite and kerosene. The influence of the surfactant (oleic acid) can be neglected as its heat capacity equals that of kerosene [16].

The thermal conductivity λ was determined via the heat flux density $\dot{q}$ measured in the conductive state without applied magnetic field for both directions of the temperature gradient: $\lambda = q \cdot d/\Delta T$. With these data, a calculation of the thermal diffusivity $\kappa = \lambda/(\rho \cdot C_p)$ within an acceptable range of error of $\pm 9\%$ was possible.

All magnetic properties were measured with a Lake Shore vibrating sample magnetometer (VSM) equipped with a temperature control unit. The pyromagnetic coefficient $K = \delta M/\delta T|_{Hi=\mathrm{const}}$ Fig. 4 was calculated with a linear fit of the magnetization between 283 K and 343 K. The susceptibility is defined similarly to the one of Finlayson [1] as $(\delta M/\delta H_i)_{T=313\,\mathrm{K}}$ of the measured magnetization curve. The factor M_3 mentioned section 1 is $M_3 = 1.45$ for $H_i = 1.1\ \mathrm{kA/m}$ and $M_3 = 1.34$ for $H_i = 14.9\ \mathrm{kA/m}$ for the EMG 905-fluid and is constant $M_3 = 1$ for the NF4000C-fluid.

From the magnetization curves a particle size distribution was calculated according to Chantrell et al. [17] which is shown in Fig. 5. It indicates that the particles in the EMG 905- and APG 513A-fluid are rather similar with mean diameters of $d_{0.5} = 9.5\ \mathrm{nm}$ and $d_{0.5} = 9.1\ \mathrm{nm}$ respectively, whereas the NF4000C-fluid has a smaller mean diameter of $d_{0.5} = 5\ \mathrm{nm}$ and a narrower particle size distribution.

The deviation of $\bar{d}$ as presented in Table 1 from the values of $d_{0.5}$ presented here is a result of the ansatz of the Langevin function, being the base of the calculation of $\bar{d}$ assuming a monodisperse particle size distribution. The TEM image of the EGM905-fluid in Fig. 6 is used for visualizing purposes only. No conclusion such as size distribution or pattern formation can be drawn from it, since the preparation steps necessary might have an impact here.

Table 1
Properties of the investigated fluids at 313 K if not stated otherwise. The mean diameter $\bar{d}$ was calculated with the Langevin-function approximating the measured curve of magnetization. Data for APG 513A-fluid from [6].

Property	Unit	EMG 905	NF4000C	APG 513A
ϕ	%	7.6 ± 1%	5.3 ± 2%	6.6
$\bar{d}$	nm	12.7 ± 1%	8.6 ± 2%	12.9
M_S (289 K)	kA/m	34.2 ± 1%	23.9 ± 2%	28.5
ρ	kg/m³	1323 ± 0.1%	1158 ± 0.1%	1345
β	1/K	7.52×10^{-4} ± 1%	8.17×10^{-4} ± 1 %	6.40×10^{-4}
C_p	J/kg K	1644 ± 7%	1727 ± 7%	
λ	W/m K	0.235 ± 5%	0.229 ± 6%	
κ	m²/s	1.08×10^{-7} ± 9%	1.15×10^{-7} ± 9%	1.1×10^{-7}
η	mPa	10.01 ± 1%	6.55 ± 0.5%	84

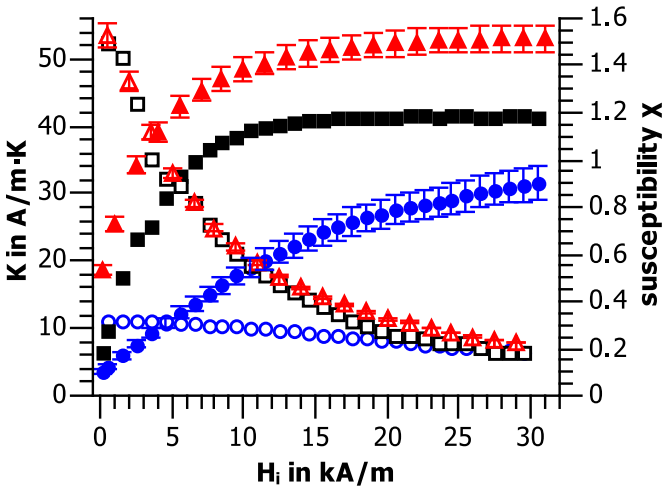

Fig. 4. Field dependence of the pyromagnetic coefficient K (full symbols) and susceptibility χ (open symbols) of EMG 905-fluid (▲), NF4000C-fluid (●) (both own measurements) and APG 513A-fluid (□) [6].

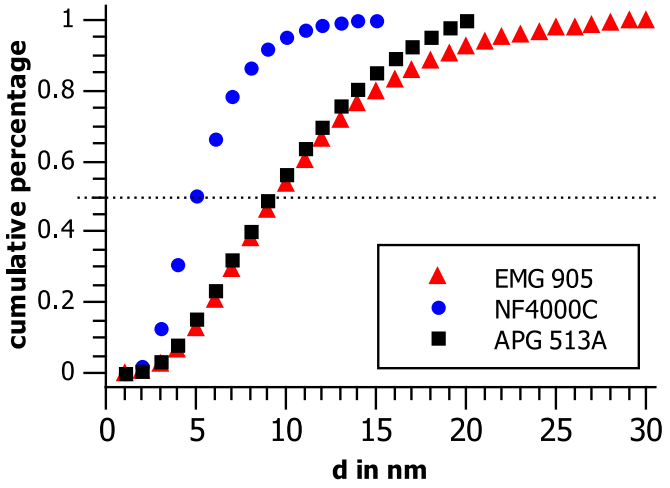

Fig. 5. Particle size distribution calculated according to Chantrell et al. [17].

The viscosity in Fig. 7 was determined with a shear rate controlled Anton Paar rheometer (Physica MCR301) using a solvent trap filled with kerosene. The APG 513A-fluid has a dynamic viscosity of 84 mPa s at 313 K [8], which is about one order of magnitude larger than that of the kerosene-based magnetic fluids investigated here. None of the fluids shows a magnetic-field-dependent viscosity.

4. Results

The heat flux density through a layer of EMG 905-fluid of a thickness of 2 mm is displayed in Fig. 8 as a function of the temperature difference for various values of the inner magnetic field strength in the layer. For a better visualization only characteristic measurements are shown here. It can be seen that in case of a positive temperature gradient (heated from below, Fig. 8a) all curves deviate at a critical temperature difference which decreases with increasing magnetic field between $\Delta T_c = 23.1\ \mathrm{K}$ for $H_i = 0\ \mathrm{kA/m}$ and $\Delta T_c = 11.4\ \mathrm{K}$ for $H_i = 14.9\ \mathrm{kA/m}$. This point of transition, according Section 2 (Experimental setup), is defined as the onset of convection and is determined via the intercept of two linear fits in the conductive and convective section of heat

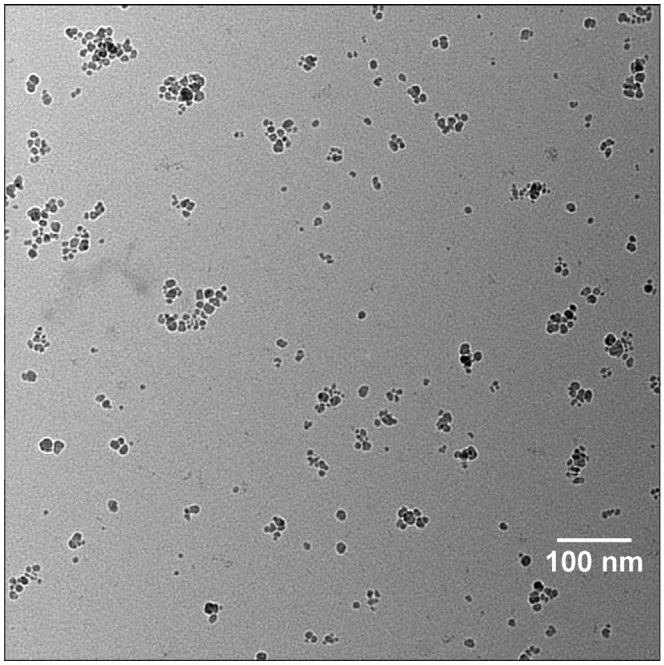

Fig. 6. TEM image of the EMG905, which is only used for the purpose of visualizing the particles.

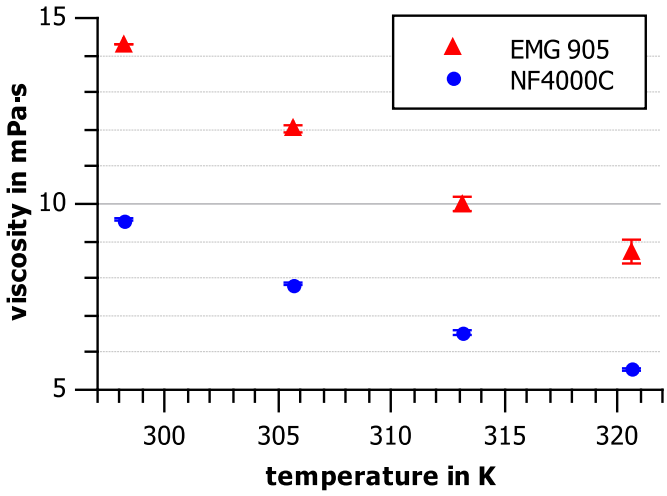

Fig. 7. Temperature dependence of the dynamic viscosity of the two kerosene-based magnetic fluids. The experimental error is determined as span of a series of repeated measurements on viscosity.

transport.

For a layer of fluid heated from above (negative temperature gradient), the transition from conduction to convection only takes place in the presence of magnetic fields as shown in Fig. 8b. This is reasonable as the buoyancy force stabilizes the layer in this setup. For the same reason the point of transition for a given magnetic field when heated from above is always found at higher absolute temperatures in comparison with the critical absolute temperature differences for positive temperature gradients.

Many of the displayed curves have been reproduced with a fresh filling of magnetic fluid in a newly assembled and calibrated measurement cell and at different points in time being 6 months apart. The deviation of the reproductive measurements from the original ones lies within the size of the symbols of the curves in Fig. 8 and is therefore not shown there.

The NF4000C-fluid shows a similar behavior. The heat flux density for a layer thickness of 2.7 mm of this fluid is presented in Fig. 9. For a positive temperature gradient, the measurements of this fluid have been performed with a temperature step of 0.5 K each 35 min for reasons of the small critical temperature difference between $\Delta T_c = 7.5$ K for $H_i = 0$ kA/m and $\Delta T_c = 5.7$ K for $H_i = 22.3$ kA/m. It was experimentally proven that this change in the measurement regime has no effect on the results.

For a negative temperature gradient, the same step width as for the EMG 905-fluid was used (i.e. 1 K). In this case the critical temperature difference is -19 K for the highest possible magnetic field strength of $H_i = 22.3$ kA/m.

A different batch of a similarly composed NF-fluid used in former measurements tended to become more viscous if used under varying temperature conditions. The manufacturer assumed a polymerization process taking partly place among excess surfactant molecules. For that reason the NF4000C-fluid was tested experimentally for the same phenomenon. Carrying out the convection measurements for different magnetic field strengths indicated a non-reproducibility of the data until both cell boundaries had been exposed to the highest temperature present during the experiments for positive and negative temperature gradients. After that a highly viscous layer of fluid was found on the cell's boundaries, and from then on, measured data could be easily reproduced with the same precision as for the EMG-fluid measurements. The layer is therefore assumed constant during the measurement cycles that followed. For that reason after filling the convection cell with a new sample, the cell was heated up to the maximum temperature of 348 K prior to the convection experiments while calibrating the thermistors.

In order to calculate realistic Rayleigh numbers, an effective layer thickness of 2.7 mm was used instead of the distance between the copper plates being 3.1 mm. It is noted here that the probably forming of a NF4000C-coating of 0.2 mm on each boundary is assumed not to have an influence on the convective motion in the layer. Theoretical investigations of Recktenwald and Lücke [18] investigate the influence of boundaries with finite thermal conductivity. They describe the boundaries by the ratio of the boundary's thickness and half the fluid layer's height being denoted δ, and the conductivity factor by the quotient of the boundary's and the fluid's thermal conductivity being denoted ζ. Here δ equals 0.15 and ζ equals 1. Comparing these values with the theoretical results [18] and their validation with experimental data [4,19], it can be supposed that the influence of the potential coating of the boundaries is not experimentally detectable.

The slope of the curves in the conductive state of fluid is dependent on the magnetic field for as well negative as positive temperature gradients. This implies that the thermal conductivity is a function of the magnetic field, and is rising with increasing field strength. A similar behavior has been measured for example by Krichler et al. [20]. However, to simplify the calculations, the thermal conductivity shown Section 3 (Fluid characterization) is measured without magnetic field and will be used further on.

A summary of all measured critical temperature differences is shown Fig. 10 as a function of the inner magnetic field strength. The theoretical predictions of Finlayson [1] are shown as dashed lines and calculated on basis of (4) for the fluid parameters of EMG 905, $d = 2$ mm, $Ra_c = 1708$ and $Ra_{m,c}$ is assumed to be 2520 for $(1+\chi) = 1.8$ and $M_3 = 1.4$.

Ra and Ra_m have been calculated for the measured data as well as for the results of Schwab [4] and Engler [6–8] and are presented Fig. 11. It is possible to determine Ra_c and $Ra_{m,c}$, which are presented Table 2, with a linear fit of the measured data and (3). Results of the experiments with a positive (negative) temperature gradient are thereby found at $\mathrm{Ra} > 0$ ($\mathrm{Ra} < 0$).

From the data of Schwab [4] none of these values can be extracted. Schwab [4] did not conduct an explicit fluid characterization within his work, he rather used an implicit method to

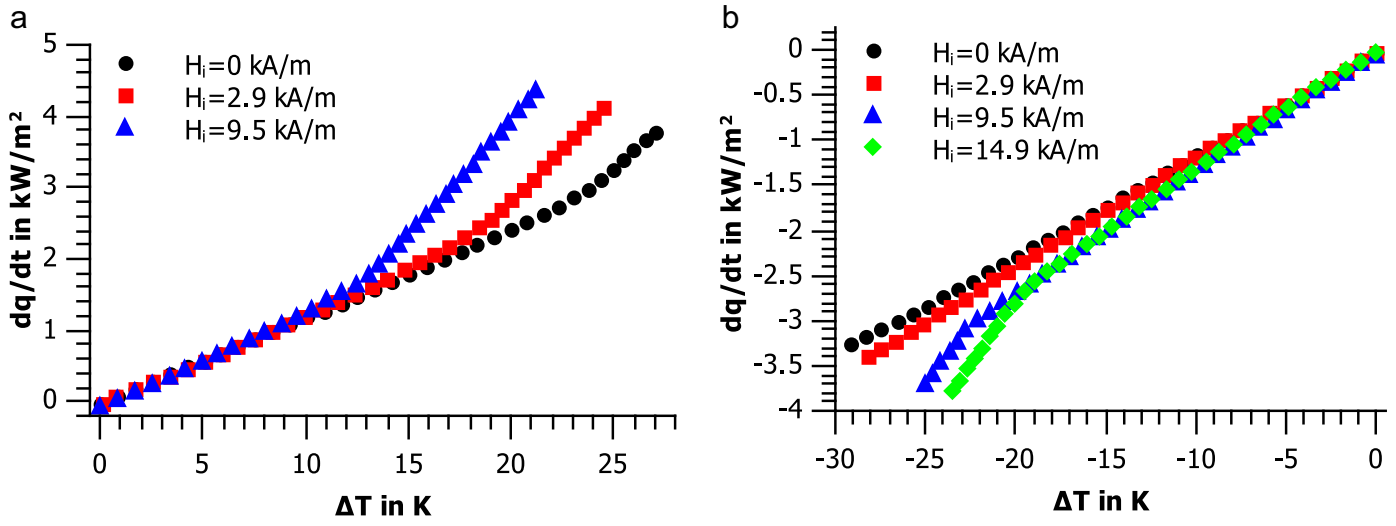

Fig. 8. Heat flux density $\dot{q}$ through a 2 mm layer of EMG 905-fluid when heated from below (a) and above (b) for various inner magnetic field strengths H_i. Deviation from reproductive measurements lies within the size of the symbols.

detect the fluidic impact from the critical temperature difference in the convection experiments. Therefore he introduced two parameters namely

$$c_a' = \frac{g\rho\beta}{\kappa\nu} \tag{5}$$

and

$$c_m' = \frac{\mu_0 K^2}{\kappa\nu(1+\chi)} \tag{6}$$

summing up all fluid-specific terms from the analytical description of the Rayleigh numbers. The latter then accordingly become

$$Ra_c = c_a' \Delta T_c \cdot d^3 \tag{7}$$

and

$$Ra_{m,c} = c_m' \Delta T_c^2 \cdot d^2. \tag{8}$$

The experimental values for EMG 905-fluid measured in this work explicitly yield $(()_{HM})$

$$c_{aHM}' = \frac{9.81\ \mathrm{m/s^2}\cdot 1328\ \mathrm{kg/m^3}\cdot 7.52\cdot 10^{-4}\ \mathrm{1/K}}{1.08\cdot 10^{-7}\ \mathrm{m^2/s}\cdot 0.011\ \mathrm{kg/s\cdot m}} = 8.21\ \mathrm{K^{-1}mm^{-3}} \tag{9}$$

and

$$c'_{mHM} = \frac{1.26\cdot 10^{-6}\ \mathrm{Vs/Am}\cdot(50.4\ \mathrm{kA/m})^2}{1.08\cdot 10^{-7}\ \mathrm{m^2/s}\cdot 0.011\ \mathrm{kg/s}(1+0.48)} = 1.8\ \mathrm{K^{-2}mm^{-2}} \tag{10}$$

for a temperature of 308 K. Schwab [4] instead used the critical temperature difference and the critical Rayleigh number $Ra_c = 1708$ to determine $(()_{LS})$

$$c_{aLS}' = \frac{1708}{14.2\ \mathrm{K}\cdot(1.5\ \mathrm{mm})^3} = 35.5\ \mathrm{K^{-1}mm^{-3}}. \tag{11}$$

The fluid parameters which enter the equation can be held constant, since the mean temperature within the convection experiment is constant throughout all experiments. For the magnetic parameter on the contrary the dependence on the magnetic field is more significant and has to be taken into account by [4]

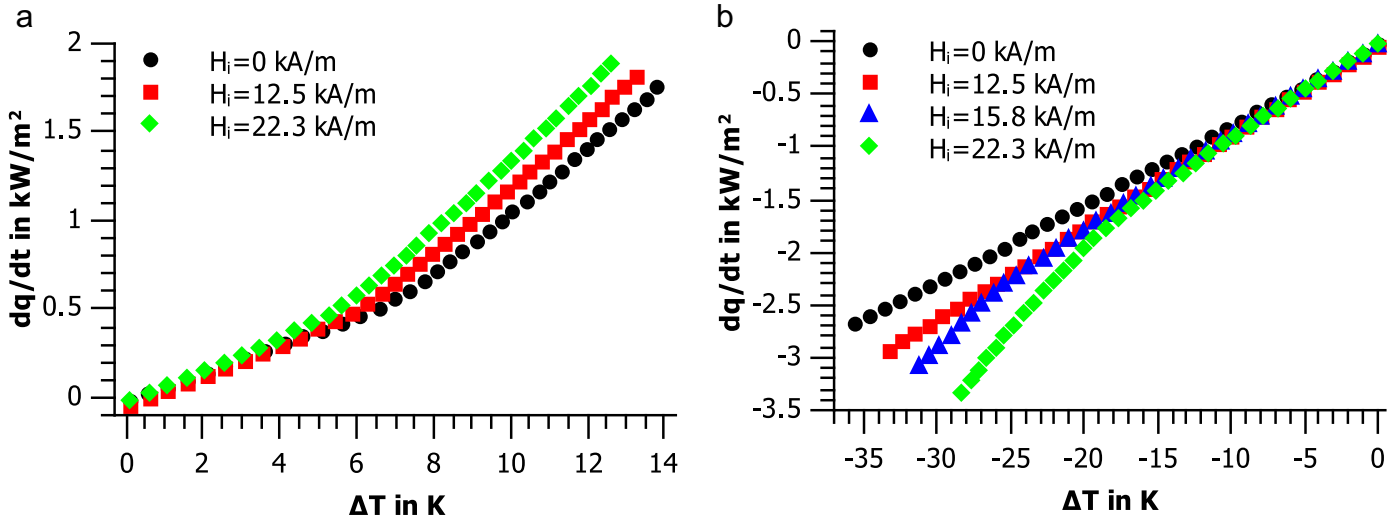

Fig. 9. Heat flux density $\dot{q}$ through a layer of NF4000C-fluid of a thickness of 2.7 mm when heated from below (a) and above (b) for various inner magnetic field strengths H_i. Temperature step was 0.5 K for (a) and 1 K for (b) each 35 min. Deviation from reproductive measurements lies within the size of the symbols.

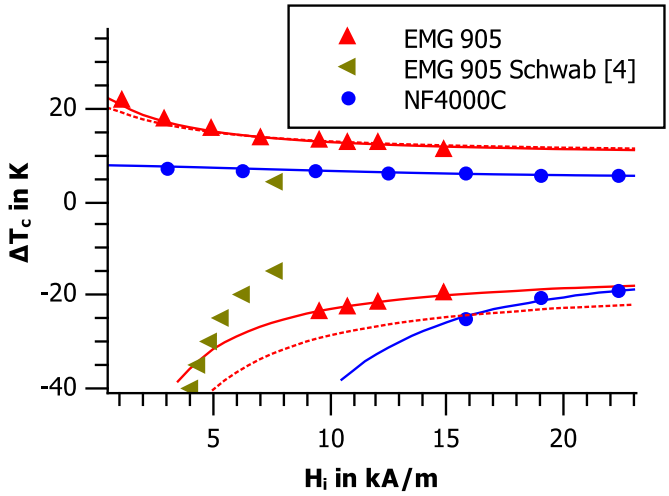

Fig. 10. Critical temperature difference ΔT_c across the layer of fluid for the onset of convection as a function of the magnetic field strength H_i. Layer thickness is 2 mm for EMG 905-fluid and 2.7 mm for NF4000C-fluid. Calculated ΔT_c are presented as blue lines for the measured fluid parameters and critical Rayleigh numbers of EMG 905 and as red lines for the NF4000C-fluid. Dashed lines are based on theoretical critical Rayleigh numbers for the EMG 905-fluid according to Finlayson [1]. Error bars are smaller than the size of the symbols. (For interpretation of the references to color in this figure caption, the reader is referred to the web version of this paper.)

$$c'_{\mathrm{mLS}} = c_{\mathrm{m}}\left(\frac{H_{\mathrm{i,c}}}{H_{\mathrm{s}}}\right)^2 \cdot \left(1 - \frac{1}{2}\left(\frac{H_{\mathrm{i,c}}}{H_{\mathrm{s}}}\right)^2\right)$$
$$= 29\ \mathrm{K^{-2}mm^{-2}} \cdot 0.092$$
$$= 2.7\ \mathrm{K^{-2}mm^{-2}} \qquad (12)$$

with $H_{i,c} = 0.5 \cdot H_c$ denotes the critical inner magnetic field strength and $H_s = 13.5$ kA/m the calculated magnetic field, where one third of the saturation magnetization of EMG 905 is reached. The parameter c_m is finally obtained by the critical point of the convection experiments by fitting the calculated nonlinear relationship of Ra and Ra_m to the experimental magnetic data. This leads to c_m being 29 $\mathrm{K^{-2}mm^{-2}}$. This procedure explains the good fit of Schwab's data [4] with the theoretical prediction Fig. 11, as well as the discrepancy Fig. 10, in which the theoretical prediction (dashed lines) was calculated for the measured parameters of the EMG 905-fluid Table 1. The comparison of the measured data within this work leading to c'_a and c'_m with the implicit data of Schwab [4] shows to which extent Schwab's assumptions can be regarded accurate. The assumed magnetic parameter is thereby much closer to the measured one than the assumed non-magnetic parameter to the measured equivalent.

Table 2
Critical thermal and magnetic Rayleigh numbers calculated on basis equation (3).

Fluid	Ra_c	$Ra_{m,c}$
EMG 905	2082	1998
NF4000C	1925	856

5. Discussion

Three magnetic fluids were analyzed in this work, having similar characteristics in pairs. The EMG 905- and the APG 513A-fluids, which are until now the best investigated fluids concerning thermomagnetic convection, possess quiet similar magnetite particles, as demonstrated in Fig. 5, but a different carrier liquid being kerosene and a higher viscous synthetic ester respectively. The NF4000C-fluid however, shows a distinct particle size distribution yet being based on kerosene as well as the EMG 905-fluid.

Fig. 11 gives rise to the assumption, that the viscosity and further parameters of the carrier liquid are not important for the critical Rayleigh numbers, as the behavior of the kerosene-based EMG 905-fluid is quite similar to the ester-based APG 513A-fluid. The NF4000C however shows a quite different trend with a much smaller critical magnetic Rayleigh number than predicted (Table 2). This fluid's composition is similar to the EMG 905-fluid but its volume concentration of magnetite is lower (5.3 % instead of 7.6 %) and its particle size distribution is different with a smaller mean diameter of $\bar{d} = 8.6$ nm. As the concentration of magnetite varies between APG 513A- and EMG 905-fluid as well, it is assumed that the change in particle size ($\bar{d}$) and particle distribution cause the unexpected behavior.

When discussing the critical Rayleigh numbers obtained by a linear fit, one has to keep in mind that these values themselves are, according to Finlayson [1], dependent on the magnetic field, which has the largest effect on small fields. Furthermore it is clear that the large gap between the data for a positive and a negative temperature gradient dominates the results of the fit.

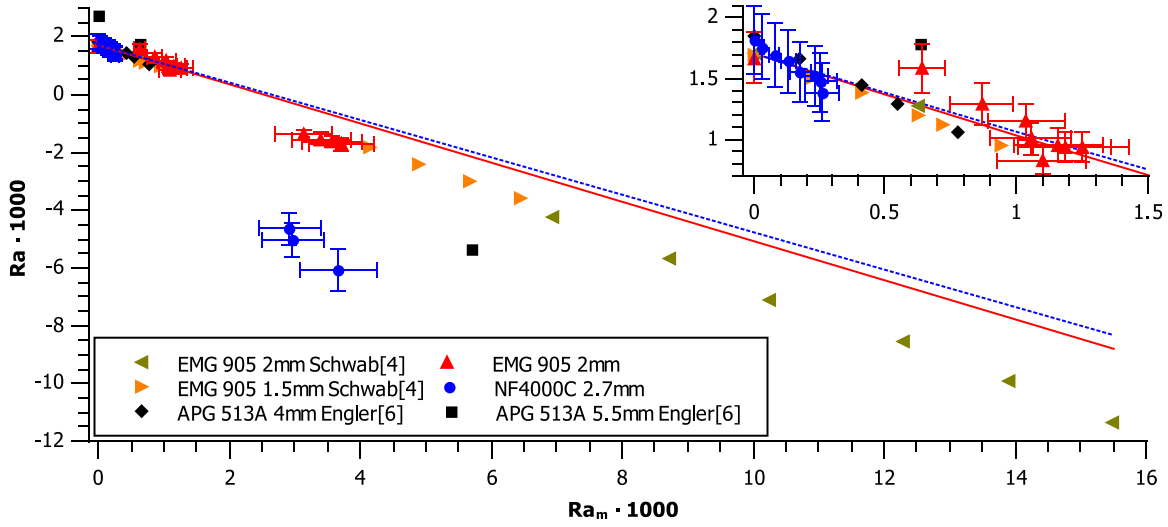

Fig. 11. Ra as a function of Ra_m including data measured by Schwab [4] and Engler [6–8] with unpublished results [21]. The lines are calculated based on Finlayson [1] for EMG 905 (solid red) and NF4000C (dashed blue). (For interpretation of the references to color in this figure caption, the reader is referred to the web version of this paper.)

There are many combinations of Rayleigh-number and magnetic Rayleigh-number that do not lead to convection. The influence of the behavior between several points in one setup is quiet insignificant.

This is insofar important as it is not yet experimentally confirmed that the same critical parameters are valid for a layer of fluid heated from above and from below. The data of Schwab lead to that assumption as they are completely linear, but they represent only one special fluid. With the present experimental setup, it is not practical to analyze the results separately for the two directions of the temperature gradient because measurements in a large range of Rayleigh numbers are necessary to compensate the quite high experimental error of each individual Rayleigh number.

To give further insight into thermomagnetic convection and its influencing parameters, further experimental data has to be obtained varying certain fluid parameters. We suggest two different paths. The first one is to conduct the exact same experiments as presented here but for a different NF4000 fluid, either having a higher or lower particle volume concentration to support the assumption that particle size distribution plays a major role in the onset of thermomagnetic convection. These experiments, according to the present results, should lead to very similar critical Rayleigh numbers. The second path is to investigate the influence of a change in the boundaries' thermal conductivity. As already mentioned in the results section, it is possible that the layer of NF4000C-fluid which forms at the boundaries due to the temperature influence does not only reduce the overall height of the layer but might also decrease the critical Rayleigh numbers to a certain extent. To analyze if this plays a major role in reducing the experimentally determined critical magnetic Rayleigh number for the NF4000C-fluid, experiments will be carried out, coating the layers' boundaries and redoing the experiments with the EMG905-fluid.

Acknowledgments

The authors especially thank Kuldip Raj from Ferrotec for the support with the fluid samples. The financial support by the Deutsche Forschungsgemeinschaft in project LA 1182/3 is gratefully acknowledged.

References

[1] B.A. Finlayson, Convective instability of ferromagnetic fluids, J. Fluid Mech. 40 (1970) 753–767.
[2] S. Odenbach, Microgravity experiments on thermomagnetic convection in magnetic fluids, J. Mag. Mag. Mater. 149 (1995) 155–157.
[3] S. Chandrasekhar, Hydrodynamic and Hydromagnetic Stability, Oxford University Press, 1961.
[4] L. Schwab, Konvektion in Ferrofluiden, Ludwig-Maximilians-Universität München, Diss, 1989.
[5] L. Schwab, U. Hildebrandt, K. Stierstadt, Magnetic Bénard convection, J. Mag. Mag. Mater. 39 (1983) 113–114.
[6] H. Engler, Parametische Modulation thermomagnetischer Konvektion in Ferrofluiden, Technische Universität Dresden, Diss, 2010.
[7] H. Engler, S. Odenbach, Parametric modulation of thermomagnetic convection in magnetic fluids, J. Phys.: Condens. Matter 20 (2008) 204135. http://dx.doi.org/10.1088/0953-8984/20/20/204135.
[8] H. Engler, A. Lange, D. Borin, S. Odenbach, Hindrance of thermomagnetic convection by the magnetoviscous effect, Int. J. Heat Mass Transf. 60 (2013) 499–504. http://dx.doi.org/10.1016/j.ijheatmasstransfer.2012.10.049.
[9] B. Huke, M. Lücke, Roll, square, and cross-roll convection in ferrofluids, J. Mag. Mag. Mater. 289 (2005) 264–267. http://dx.doi.org/10.1016/j.jmmm.2004.11.075.
[10] D. Laroze, P.G. Siddheshwar, H. Pleiner, Chaotic convection in a ferrofluid, Commun. Nonlinear Sci. Numer. Simul. 18 (2013) 2436–2447. http://dx.doi.org/10.1016/j.cnsns.2013.01.016.
[11] B.M. Berkovsky, V.E. Fertman, V.K. Polevikov, S.V. Isaev, Heat transfer across vertical ferrofluid layers, Int. J. Heat Mass Transf. 19 (1976) 981–986.
[12] G. Fanselau, Die Erzeugung weitgehend homogener Magnetfelder durch Kreisströme, Z. Phys. 54 (1929) 260–269.
[13] E.F. Westrum, F. Grønvold, Magnetite (Fe_3O_4) heat capacity and thermodynamic properties from 5 to 350 K, low temperature transition, J. Chem. Thermodyn. 1 (1969) 543–557.
[14] H.W. Deng, K. Zhu, G.Q. Xu, Z. Tao, C.B. Zhang, G.Z. Liu, Isobaric specific heat capacity measurements for kerosene RP-3 in the near-critical and supercritical regions, J. Chem. Eng. Data 57 (2011) 263–268. http://dx.doi.org/10.1021/je200523a.
[15] M. Higano, A. Miyagawa, K. Saigou, H. Masuda, H. Miyashita, Measuring the specific heat capacity of magnetic fluids using a differential scanning calorimeter, Int. J. Thermophys. 20 (1) (1999) 207–215.
[16] F.O. Cedeño, M.M. Prieto, J. Xiberta, Measurements and estimate of heat capacity for some pure fatty acids and their binary and ternary mixtures, J. Chem. Eng.Data 45 (2000) 64–69.
[17] R.W. Chantrell, J. Popplewell, S. Charles, Measurements of particle size distribution parameters in ferrofluids, IEEE Trans. Mag. MAG-14 (5) (1978) 975–977.
[18] A. Recktenwald, M. Lücke, Thermoconvection in magnetized ferrofluids: the influence of boundaries with finite heat conductivity, J. Mag. Mag. Mater. 188 (1998) 326–332.
[19] P.J. Stiles, M. Kagan, Thermoconvective instability of a horizontal layer of ferrofluid in a strong vertical magnetic field, J. Mag. Mag. Mater. 85 (1990) 196–198.
[20] M. Krichler, S. Odenbach, Thermal conductivity measurements on ferrofluids with special reference to measuring arrangement, J. Mag. Mag. Mater. 326 (2013) 85–90. http://dx.doi.org/10.1016/j.jmmm.2012.08.037.
[21] H. Engler, Private Communication, August 2014.